RESEARCH ARTICLE

PREPARATION AND APPLICATION OF B-CYCLODEXTRIN POLYMERIZED WITH PHENOL-FORMALDEHYDE AS AN ADSORBENT FOR THE REMOVAL OF PB(II) AND HG(II) FROM AQUEOUS MEDIA

[1]Krishnan, N. P., [2]Ilayaraja, M., [3]Muthukrishnan, P. and [4],*Sayee Kannan, R.

[1]Department of Chemistry, K.L.N College of Engineering, Pottapalayam-630612, India
[2]Department of Chemistry, SBM College of Engineering & Technology, Dindigul-624005, India
[3]Department of Chemistry, Faculty of Engineering, Karpagam University, Coimbatore-64102, Tamilnadu, India
*[4]PG & Research Department of Chemistry, Thiagarajar college, Madurai-625009, India

ARTICLE INFO	ABSTRACT
	The Phenol-Formaldehyde/β-cyclodextrin (β-CD) resin (PFCR) adsorbent with macro cycle network structure showed superior adsorption properties for Hg (II) and Pb (II) ions. FT-IR spectral analysis before and after Hg(II) and Pb(II) adsorption represented that the functional groups responsible for Hg(II) and Pb(II) adsorption. Thermodynamic studies revealed that Hg (II) and Pb (II) adsorption on the PFCR adsorbent is a favorable, spontaneous, and endothermic chemisorption process. The binding force between Hg (II) and Pb (II) ions and functional groups has been strengthened at high temperatures, which made the adsorption more favorable at high temperatures. The adsorption process fitted well by the Temkin isotherm for Pb(II) ion and both the metal ions fitted well with Jovanoic isotherm models. This study will contribute to an in-depth understanding of adsorption phenomena, and provide a base for the scientific and engineering practical applications of the PFCR adsorbent.

INTRODUCTION

Most of the metals are known to be toxic and half of these, including cadmium, chromium, copper, lead, mercury, nickel, selenium, silver and zinc, are released into the environment in quantities that pose a risk to human health (Ireland *et al.,* 1991). Heavy metal contamination exists in aqueous waste streams from diverse industries such as metal plating, manufacturing, batteries, as well as agricultural sources where fertilizers and fungicidal sprays are intensively used. Cu, Zn, Hg, and Cd are harmful wastes produced by industry that pose a risk of contamination groundwater and other water resources. Heavy metals are not biodegradable and tend to accumulate in living organisms, causing various diseases and disorders (Guo *et al.,* 2002; Albert *et al.,* 1995; Nuhoglu *et al.,* 2002; Ngah *et al.,* 2002). Lead is an important compound used as an intermediate in processing industries such as plating, paint and dyes, glass operations, and lead batteries (Aroua *et al.,* 2008).

*Corresponding author: Sayee Kannan, R.
PG & Research Department of Chemistry, Thiagarajar college, Madurai-625009, India

However, the presence of lead in water even at a very low level would be harmful to aquatic life and human health in terms of its toxicological, potential carcinogenic and neurotoxical effects (Martins *et al.,* 2006). The permissible limits of lead in drinking water and surface water intended for drinking, as set by EU, USEPA and WHO, are 0.010, 0.015 and 0.010 mg l^{-1}, respectively (Balaria *et al.,* 2008). Mercury has a high tendency of binding with proteins and it mainly affects the renal and nervous systems (Denizli *et al.,* 2003). Therefore, reliable methods are necessary for the removal of heavy metals from aquatic environment.

A great deal of effort has been devoted to the effective removal of heavy metal ions from environmental matrices. Various treatment techniques available for the removal of toxic metals are adsorption, chemical precipitation, ion exchange, coagulation, reverse osmosis, electrolysis and membrane process, etc. (Merzouka *et al.,* 2008; Meunier *et al.,* 2006; Mohamed *et al.,* 2008). However, among all these methods, adsorption is considered an effective, efficient and economic method for the removal of pollutants from wastewater (Feng *et al.,* 2010; Gupta *et al.,* 2012; Mittal *et al.,* 2008). This

technique can be applied frequently on large scale, as it can handle fairly large flow rates, producing a high quality of water without producing notorious sludge, residual contaminants, etc (Gupta *et al.,* 2007). Moreover, adsorption is universal and fast in nature and applicable for the removal of organic and inorganic pollutants even at low concentration. Recent research has focused on adsorbents such as activated carbons, zeolites, clays, biomass and polymeric materials for the removal of heavy metals (Crini, 2005).

In wastewater treatment, especially in the removal of heavy metals, natural polymers, mainly polysaccharides such as chitosan, starch and its derivatives, cyclodextrins, have attracted particular attentions, due to their physico-chemical characteristics, low cost, availability and the presence of various reactive groups on the backbone chain. Recently, we have synthesized carboxymethylated β-cyclodextrin modified magnetic nanoparticles which could remove Cu^{2+} ions effectively from water based on complexation reactions between metal ions and carboxyl group (Badruddoza *et al.,* 2011).

Cyclodextrins (CDs) are cyclic oligosaccharides consisting of 6 (α), 7 (β), 8 (ɤ) glucopyranose units linked together via α (1–4) linkages. They form a torus-shaped ring structure which contain an a polar cavity with primary hydroxyl groups lying on the outside and secondary hydroxyl groups inside (Szejtli, 1998). This renewable and biodegradable compound has the ability to complex various metal ions and this complexation ability can be improved by modifying CDs with suitable functional groups through esterification, oxidation reactions and cross-linking of hydroxyls outside the interior cavity (Norkus, 2009). Though β-CD/metal complexation has been used in water decontamination technique, particularly in the removal of heavy metals (Crini, 2006; Mahlambi *et al.,* 2010), very little attention has been paid to the adsorption selectivity of heavy metal ions on these cyclodextrin based adsorbents. In this work, for improved effect the metal complexing ability and selectivity, β-cyclodextrin polymer was synthesized and used to graft on the phenol-formaldehyde surface. The aim of this work is to study the utility of PFCR, low cost as well as non-hazardous material, as an adsorbent for Pb (II) and Hg (II) removal from aqueous solution by batch experiments. The effect of experimental parameters such as initial concentration, contact time and temperature was investigated. Furthermore, equilibrium, kinetic and thermodynamic studies on the adsorption of Pb(II) and Hg(II) onto the PFCR were also carried out for the design of adsorption process.

MATERIALS AND METHODS

Materials

The chemicals used in the present study were con. sulfuric acid (Specific gravity =1.82), formaldehyde (37-40% solution) and phenol (Density =1.057gm^{-1}). β-cyclodextrin (molecular weight, 79.87) was purchased from SRL chemicals, Mumbai, India. The Mercuric chloride ($HgCl_2$, M.W. 271.50) and Lead nitrate ($Pb(NO_3)_2$, M.W. 331.21) were obtained from RANKEM chemicals New Delhi, India. All the chemicals used were analytical grade. The double distilled (DD) water was used throughout the investigation.

Preparation of PFCR composites

Phenol and con. sulfuric acid (1:1) and 0.5 mg of β-cyclodextrin were mixed slowly with constant stirring in an ice bath. The mixture was then heated to 70°C for three hours, and was kept overnight for cooling. The product was polymerized with formaldehyde solution (12 ml) in an ice bath, and then heated to 70°C for three hours. The product was cured, and was then ground washed with DD water to remove the free acid. Then the sample was dried at 70°C for 16 h. Finally the composite resin was sieved and preserved for characterization and further studies.

Adsorption experiments

Batch mode adsorption studies were carried out by adding certain amount of adsorbent and 40 ml of metal ion solutions of certain concentrations, dose, contact time and temperatures in a thermo stated water bath shaker with a shaking of 200 rpm. The samples were withdrawn from the shaker at predetermined time intervals, and solutions were separated from the adsorbent by centrifugations at 4000 rpm for 5 min. To determine the residual metal ion concentration, the absorbance of the supernatant solution was measured before and after treatment using atomic absorption (Elico SL-173) spectrometry at wavelength of 283.3 253.7 nm for Pb(II) and Hg(II) respectively. Experiments were carried out twice and the concentrations given were average values. The initial metal ion concentration in the test solution and the contact time were varied to investigate their effect on the adsorption kinetics. The pH of the metal ion solution was adjusted by using NaOH or HCl solution and a pH meter. The adsorption studies were carried out at different temperatures (308K, 318K and 328K).This was used to determine the effect of temperature on the thermodynamic parameters. The amount of adsorption in batch experiments and adsorption efficiency were calculated as follows:

$$q= (C_o - C_e) V / m \qquad \text{...................... (1)}$$
$$\text{Efficiency (\%)} = (C_o - C_e) / C_o \times 100 \qquad \text{.........…………. (2)}$$

Where C_o is the initial concentration (mg/L), C_e is the equilibrium concentration (mg/L), V is the volume of solution (mL), m is the mass of adsorbent (g) and q is the amount of adsorbed (mg/g).

Surface characteristic of the adsorbent

Surface area and porous size distribution of PFCR sample were measured by nitrogen adsorption analysis (Quantachrome V5.02). Crystal structure of sample was determined by performing X-ray diffraction (XRD) on SHIMADZU 6000 X-ray diffraction spectrometer. Surface morphologies were examined by a scanning electron microscope (SEM, JEOL (JSM 6390) with the working distance of 9.9 mm and an accelerating voltage of 30 keV. The SEM was equipped with an energy dispersion spectrometer (EDS) and it was used to perform the analysis of chemical constituents of the adsorbent. Infrared absorption spectroscopy (IR) spectra were measured at room temperature on a Fourier transform infrared (FTIR) spectroscopy (8400s SHIMADZU spectrometer) using the KBr pellet technique. Thermo gravimetric analysis (TGA) was

carried out using a Shimadzu TGA Q50, with a heating rate of 20 ˚C min^{-1}, under nitrogen flow at rate of 60 mL min^{-1}.

RESULTS AND DISCUSSION

BET

The specific surface area was determined using the BET equation applied to the adsorption data. The surface area of PFCR was found to be 18.06 m[2]/g. Total pore volume is 7.25 cm[3]/g and pore size is 248.7 A° in Fig.1. PFCR has a relatively promising surface area although it was obtained from β-cyclodextrin.
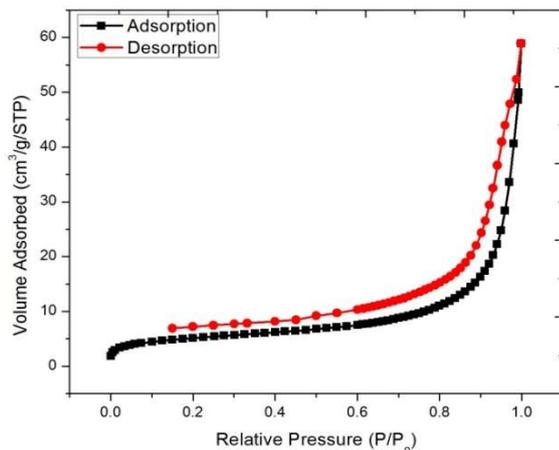

Fig.1. Adsorption-desorption isotherms of nitrogen at 77 K on PFCR

FTIR

FTIR spectra of the β-CD, PFCR, PFCR-Hg(II) and PFCR-Pb(II) are shown in Fig.2. The main bands are observed in the IR spectra of β-CD, in Fig.2a. FTIR data of β-CD shows that characteristic bands at 3246.2, 1640.8 1412.0, 892 cm^{-1} and 1172.1cm^{-1} correspond to the free OH, C=O, CH_2, C=CH_2 and C-O-C stretching vibrations respectively. Fig.2b shows the FTIR spectrum of PFCR. The absorption peak at 3150.3 cm^{-1} indicates the presence of OH groups on the surface of PFCR. The characteristic bands at 1637.1 cm^{-1} and 1462.5 cm^{-1} correspond to the C=O and C-CH_2 stretching vibrations. The band at 1025.4 cm^{-1} is attributed to the C-O-C.

FTIR data of PFCR-Hg(II) showed that characteristic bands at 3013.5, 1739.0 and 1439.0 cm^{-1} corresponding to OH, C=O and C-CH_2 stretching vibrations respectively in Fig.2c. The three new peaks were observed at 2141.8, 1366.6 and 891.4 cm^{-1} corresponding to C=C, C-CH_3 and C=CH_2 which revealed the adsorption of Hg(II) onto PFCR. FTIR data of PFCR-Pb (II) showed that characteristic band at 3190.1, 1593.0, 1459.7 and 1023.0 cm^{-1} correspond to the OH, C=O, C-CH_2 and C-O-C stretching vibrations respectively. Fig.2d. indicated that mostly the bonded OH groups, C=O stretching, C-CH_2 bending vibrations and C-O-C vibrations were involved in Pb(II) ion adsorption. There were clear band shifts and intensity increases in Fig.2d. These findings suggest that there is attachment of Pb(II) on the PFCR.
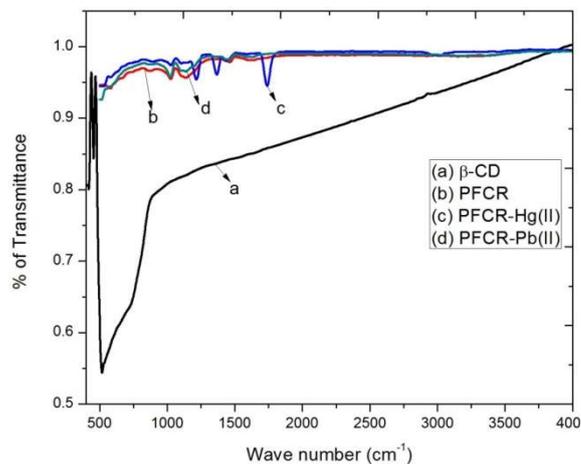

Fig.2. FTIR spectra of (a) β-CD (b) PFCR (c) PFCR- Hg(II) (d) PFCR- Pb(II)

XRD

The XRD patterns as shown in Fig.3 were performed to analyze the crystalline nature. The characteristic 20˚- 25˚ peaks of PFCR were discernible, the diffraction spectrum of PFCR did not show any obvious crystalline peak at the scan range 10-90˚ thereby indicating the amorphous phase of PFCR.
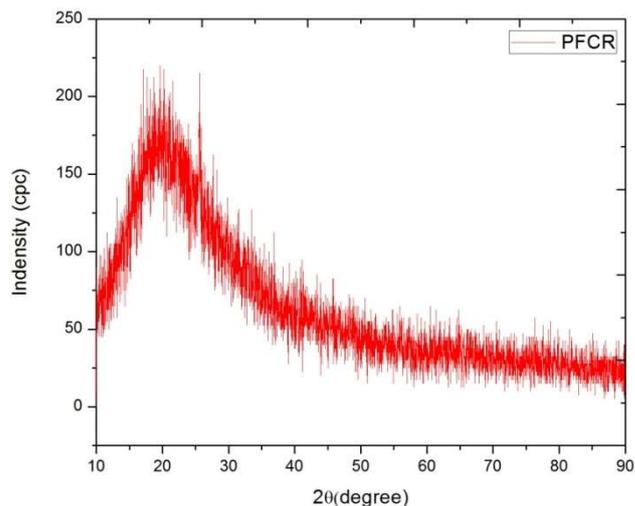

Fig.3. XRD pattern of PFCR

SEM

SEM is a primary tool for characterizing the surface morphology and fundamental physical properties of the adsorbent surfaces. It is useful for determining the particle shape, porosity and appropriate size distribution of the adsorbent. The SEM micrographs for the unloaded PFCR and Hg(II) and Pb(II) loaded PFCR are shown in Fig.4. Fig.4a indicates that the fresh adsorbent has an extensive, well pronounced and irregular distribution of pore sizes, indicating good possibility for the metals to be trapped and adsorbed. Fig.4b and Fig.4c show that micro graphs of the Hg(II) and Pb(II) loaded PFCR adsorbent had a more homogeneous and smoother surface following adsorption. It became clear from these SEM micrographs that a multilayer coverage of metal ions had adsorbed on the surface of PFCR.
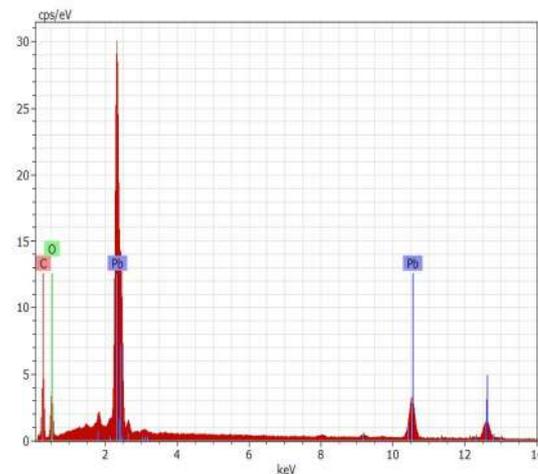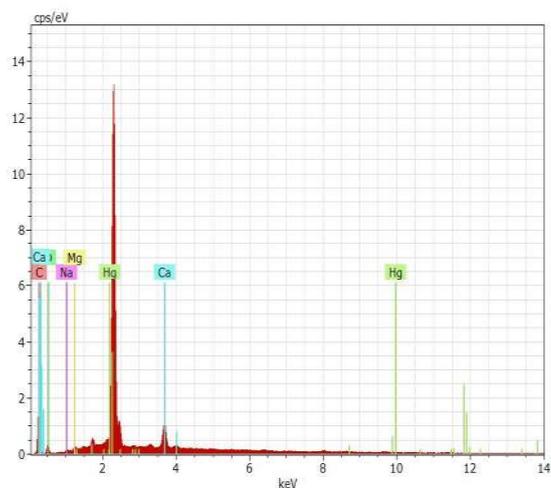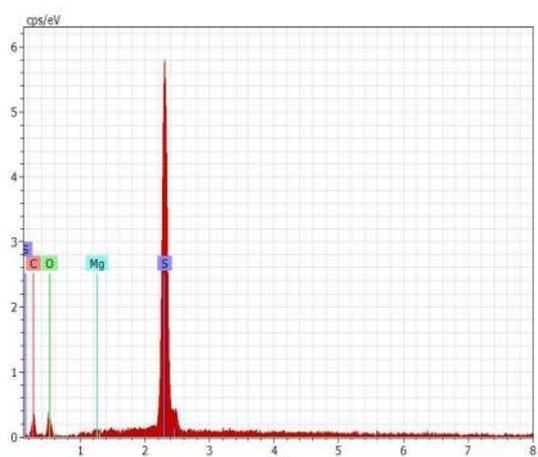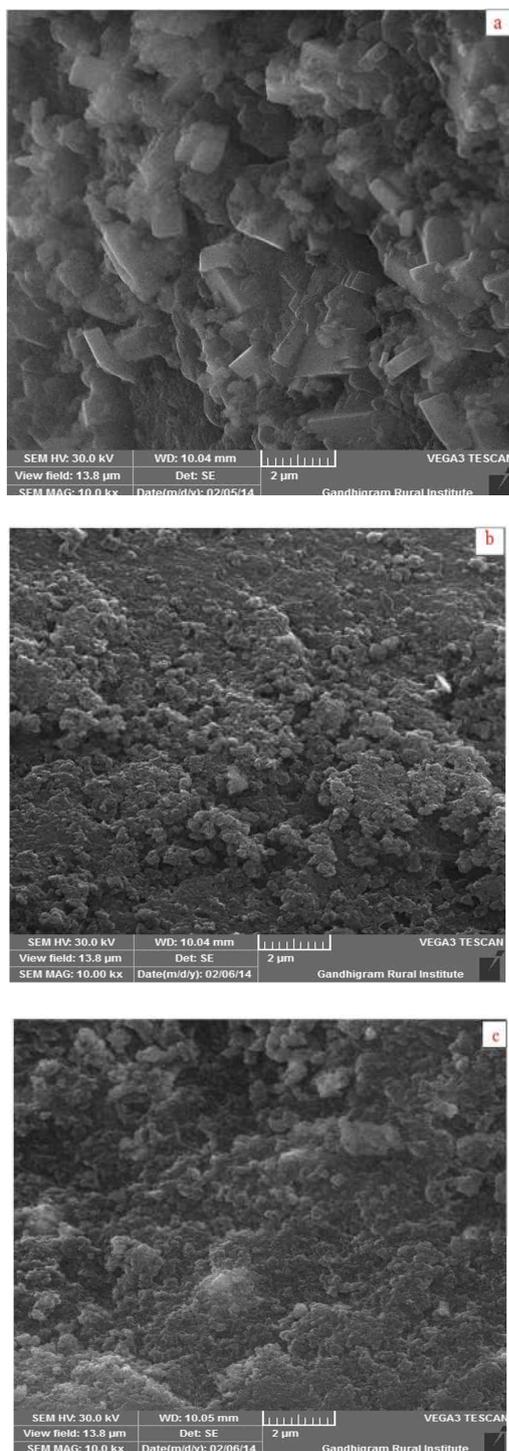
Fig.4. The SEM images of (a) PFCR (b) PFCR-Hg (II) (c) PFCR-Pb (II)

Fig.5. Energy dispersive spectra of (a) PFCR (b) PFCR-Hg (II) (c) PFCR-Pb (II)

EDX

Further confirmation of the adsorption of Hg(II) and Pb(II) on PFCR was done by energy dispersive X-ray analysis (EDX). Fig.5a for the unloaded PFCR, did not show any characteristic signal for metal ions, but only showed for the four major constituents, i.e., C, O, Mg and S. Whereas for Hg(II) and Pb(II) loaded PFCR (Fig.5b and Fig.5c) signals of presence of Hg(II) and Pb(II) were observed. This showed the diffusion or accumulation of metal ions onto the surface of PFCR.

TGA

The TGA thermogram for the PFCR sample is shown in Fig.6. The thermogravimetric profile revealed that the mass loss occurs in three stages. The first weight loss about 17.43% in the temperature range 50 - 124 °C, which may be the combined water that existed in PFCR composite. The second weight loss occurred in the temperature range 124 - 415 °C, a typically high enough temperature to induce thermal degradation of ordinary carbon polymers for about 30.01%. The final weight loss was found above 415 - 700 °C, which is about 18.87%.

Finally, no mass loss was detected when the temperature was increased above 700 °C. This result indicated that the PFCR are stable at higher temperature. The char residue of PFCR content was 35.6%.The characterization results confirmed that the formation of the adsorbent PFCR occurred successfully.
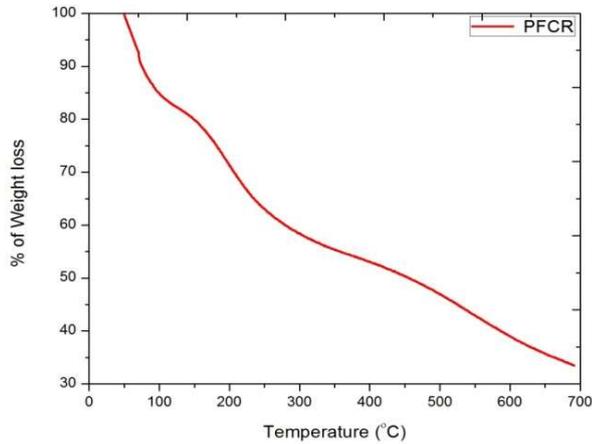

Fig.6. TGA curve of PFCR

Effect of initial concentration

Effect of initial Hg(II) and Pb(II) ion concentration was studied at different initial metal ion concentrations in the range of 10 - 50 mg/L at 298 K with 0.080 g PFCR at 120 min. The percentage of Hg(II) and Pb(II) ions adsorption at different metal concentrations using PFCR decreased with increase in metal ion concentration. This may be due to saturation of available adsorption sites onto PFCR. The effect of initial concentration on the removal of Hg(II) and Pb(II) by the adsorbent was indicated in Table.1 and Fig.7.
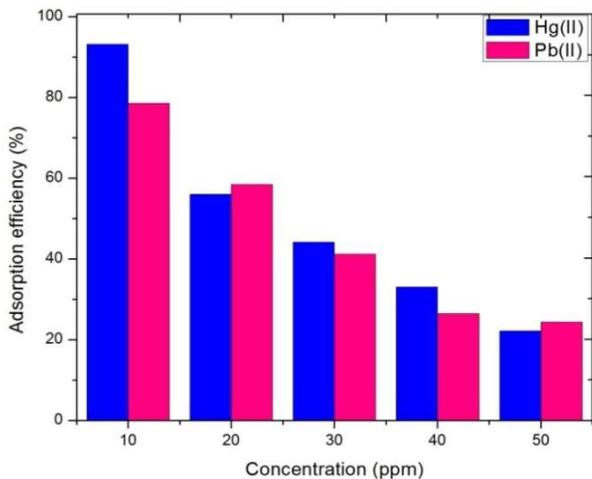

Fig.7. Effect of initial concentrations of Hg (II) and Pb (II)

Effect of contact time

The effect of contact time on the adsorption of Hg(II) and Pb(II) was at 10 mg/L. The Hg(II) and Pb(II) adsorption increased with increasing the contact time, the maximum removal of both Pb(II) and Hg(II) ions occurred at 120 min, after which there were no significant changes. The equilibrium was reached at 150 min for both the metal ions. Following this, the adsorption rate was uniform as there was no significant

change in adsorption with the increasing time. The initial fast adsorption is due to the availability of more active sites and more functional groups which participate in the lead and mercury uptake till equilibrium is attained and thereafter, there was no further adsorption. All the results are presented in Table 2 and Fig.8.
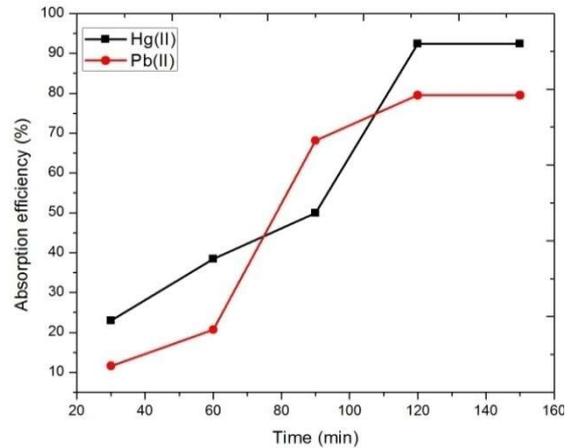
Fig.8. Effect of contact time

Effect of adsorbent mass

The effect of adsorbent dosage on lead and mercury removal was studied by varying the amount PFCR between 0.020 - 0.100 g. It is evident from Table 3 and Fig.9, that the removal of Hg(II) and Pb(II) was increased with increase in PFCR dose until a constant value was achieved. That is, the percentage removal that was increased from 26.1% to 93.6% for Hg(II) and Pb(II) was increased from 18.5% to 79.2 % as the PFCR adsorbent. This can be associated with higher available surface area and more available sorption sites at higher sorbent doses. The optimum adsorbent dosage was found to be 0.080 g for both metal ions. The adsorption efficiency of Hg(II) and Pb(II) was observed at 93.6% and 79.2% respectively.
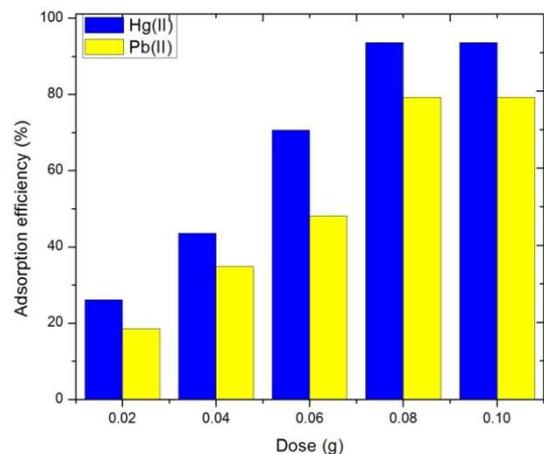
Fig.9. Effect of adsorbent dose

Adsorption isotherms

Adsorption isotherms describe qualitative information on the nature of the solute-surface interaction as well as the specific relation between the concentration of adsorbate and its degree of accumulation onto adsorbent surface at constant temperature.

Table 1. Effect of initial concentration of Hg (II) and Pb (II)

| Concentrations (ppm)	Adsorption efficiency (%)					Amount of adsorbed (q) (mg/g)				
	10	20	30	40	50	10	20	30	40	50
Hg (II)	93.2	56	44.2	33.1	22.2	117.5	85.5	69.5	54	41
Pb (II)	78.6	58.5	41.2	26.5	24.4	142	107	76.5	51	48.5

Table 2. Effect of contact time

Contact time (min)	Adsorption efficiency (%)					Amount of adsorbed (q) (mg/g)				
	30	60	90	120	150	30	60	90	120	150
Hg (II)	23.0	38.4	50.0	92.4	92.4	29.0	48.5	63.0	116.5	116.5
Pb (II)	11.6	20.7	68.1	79.5	79.5	21.0	37.5	123	143.5	143.5

Table 3. Effect of adsorbent dose

Dose (g)	Adsorption efficiency (%)					Amount of adsorbed (q) (mg/g)				
	0.020	0.040	0.060	0.080	0.100	0.020	0.040	0.060	0.080	0.100
Hg (II)	26.1	43.6	70.6	93.6	93.6	132	110	118.6	118	94.4
Pb (II)	18.5	34.9	48.1	79.2	79.2	134	126	116	143	114.4

Adsorption isotherms are critical in optimizing the use of adsorbents, and the analysis of the isotherm data by fitting them to different isotherm models is an important step to find the suitable model that can be used for design purposes. In the current study, a comparison of Langmuir, Freundlich, Temkin, D-R and Jovanoic isotherm models were fitted to analyze the equilibrium data. The linear form of Langmuir isotherm was represented by the following equation:

$$\frac{C_e}{q_e} = \frac{1}{K_L \times q_m} + \frac{C_e}{q_m} \qquad \text{............................... (3)}$$

Where q_m is monolayer (maximum) adsorption capacity (mg/g) and K_L is Langmuir constant related to energy of adsorption (1/mg) obtained from the slope and intercept values of the plot C_e/q_e against C_e respectively.

According to Hall *et al.* (1996), the essential characteristics of Langmuir isotherm can be explained in terms of dimensionless constant separation factor (R_L), which is defined by the following equation:

$$R_L = 1/1 + K_L \, C_o \qquad \text{........................... (4)}$$

Where, K_L (L/mg) is the Langmuir constant related to the energy of adsorption and C_o (mg/L) is the initial concentration of metal ions. The R_L value indicates the type of the isotherm to be either unfavorable ($R_L>1$), linear ($R_L=1$), favorable ($0<R_L<1$), irreversible ($R_L=0$).

The linear form of Freundlich isotherm equation was employed for the adsorption of Hg(II) and Pb(II) onto the PFCR adsorbents was represented by

$$\log q_e = \log K_F + 1/n \, \log C_e \qquad \text{........................... (5)}$$

Where q_e is amount of Hg(II) and Pb(II) adsorbed at equilibrium (mg/g), C_e is the equilibrium concentration of metal ion in solution (mg/l). A plot of log q_e against log C_e gives a straight line, K_F and n are constant incorporating factors affecting the adsorption capacity and intensity of adsorption calculated from the intercept and slope of the plot respectively.

The Dubinin–Radushkevich (Dubininand Radushkevich, 1947) isotherm has been used to describe the sorption of metal ions; the equation has the form:

$$\ln q_e = \ln q_m - \beta\varepsilon^2 \qquad \text{................................(6)}$$

Where q_e is the amount of Hg(II) and Pb(II) adsorbed per unit weight of adsorbent (mg/g), q_m is the maximum sorption capacity, β is the activity coefficient related to mean sorption energy, and ε is the Polanyi potential, which is equal to

$$\varepsilon = RT \ln (1+1/C_e) \qquad \text{............................. (7)}$$

Where R is the gas constant (kJ/mol K) and T is the temperature (K). The saturation limit q_m may represent the total specific microspore volume of the sorbent. The sorption potential is independent of the temperature but varies according to the nature of sorbent and sorbate.

The biosorption type based on the D-R model can be predicted by the mean free energy (kJ/mol) employing Eq.8 (Foo and Hameed, 2010):

$$E = 1/ (2\beta)^{1/2} \qquad \text{........................... (8)}$$

The magnitude of E may characterize the type of the adsorption as chemical ion exchange (E=8-16 kJ/mol), or physical adsorption (E<8 kJ/mol).

The Temkin isotherm (Temkin and Pyzhev, 1940) is given as

$$q_e = B_1 \ln K_T + B_1 \ln C_e \qquad \text{........................... (9)}$$

Where K_T (1/g) is the equilibrium binding constant, corresponding to the maximum binding energy and constant B_1 is related to heat of adsorption calculated from the intercept and slope of the plot q_e against ln C_e respectively Fig.10. The Jovanoic isotherm (Jovanoic,1969), which is based on the same assumptions of the Langmuir isotherm, also considers the possibility of some mechanical contacts between the adsorbing and desorbing molecules on the homogeneous surface and can be represented in a linear form as follows:

$$\ln q_e = \ln q_m + K_J C_e \qquad \text{..................... (10)}$$

Where, q_m is the maximum amount adsorbed (in mg/g) and K_J (in L/mg) is the constant related to the energy of adsorption. The q_m and K_J can be calculated from the intercept and slope of the linear plot of $\ln q_e$ against C_e (Fig.11). As seen from Table 4, the correlation coefficients showed that the Temkin and Jovanoic model was the best fitted in five isotherm models. Langmuir, Freundlich and Dubinin–Radushkevich models were not very good. The Jovanoic isotherm model was well described in Pb(II) onto PFCR. The maximum amount adsorbed was 5.386 mg/g for Pb(II).
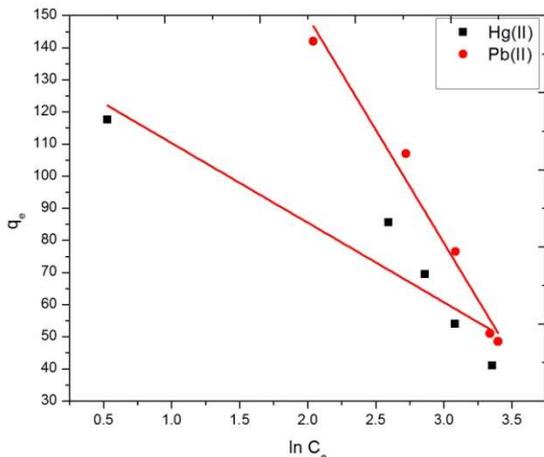

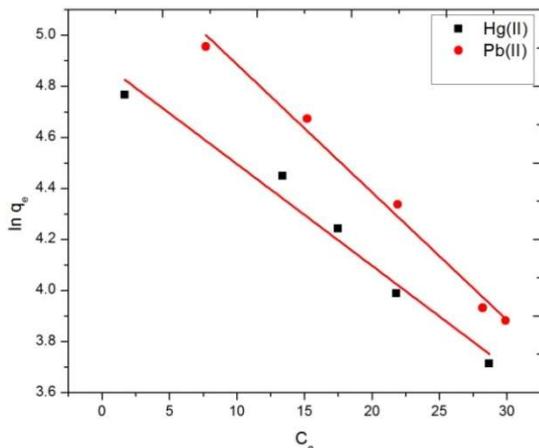**Fig.10.Temkin isotherm plots for the adsorption the of Hg(II) and Pb(II) onto PFCR**

Fig.11. Jovanoic isotherm plots for adsorption of Hg(II) and Pb(II) onto PFCR

Kinetic Studies

Designing of adsorption treatment systems requires knowledge of kinetic processes due to the many varied chemical systems, the nature of different adsorbents, and the different designs of contacting systems. For that reason, three liquid-phase adsorption kinetic models are available, namely the Lagergren pseudo-first order, pseudo-second order model and intraparticle diffusion models.

Pseudo-first order model

The Lagergren rate equation is one of the most widely used adsorption rate equations for the adsorption of solute from a liquid solution. The pseudo-first order kinetic model can be expressed by the following equation (Lagergren, 1898).

$$\ln (q_e - q_t) = \ln q_e - k_1 t \qquad \text{……………… (11)}$$

Where q_e and q_t refer to the amount of metals adsorbed (mg/g) at equilibrium and at any time, t (min), respectively, and k_1 is the equilibrium rate constant of pseudo-first order sorption (1/min).

Table 4. Different adsorption isotherm model parameters for the adsorption of Pb(II) and Hg(II) on PFCR

Mathematical models	parameters	Pb(II)	Hg(II)
	R^2	0.941	0.903
Langmuir isotherm	$K_L \times 10^2$	12.74	22.86
	q_m (mg/g)	38.46	41.66
Freundlich isotherm	R^2	0.924	0.775
	K_F	496.5×10^{-4}	104.4×10^{-3}
	n	1.246	3.154
Temkin isotherm	R^2	0.980	0.885
	B_1	70.42	24.78
	K_T	290.4	135.0
D-R isotherm	R^2	0.890	0.920
	$\beta \times 10^5$	0.600	0.700
	q_m (mg/g)	345.14	98.85
	$\times 10^{-2}$	2.88×10^{-2}	10.1×10^{-3}
	E kJ/mol		
Jovanoic isotherm	R^2	0.990	0.975
	K_J (L/mg)	0.050	0.039
	q_m (mg/g)	5.386	4.893

The slope and intercept of the plot of $\log (q_e - q_t)$ versus t are used to determine the first order rate constant, k_1. It was found that the correlation coefficient (R^2) had low value (<97%). The pseudo-first order model is inapplicable to describe the kinetics of Hg(II) and Pb(II) by adsorption using PFCR adsorbents.
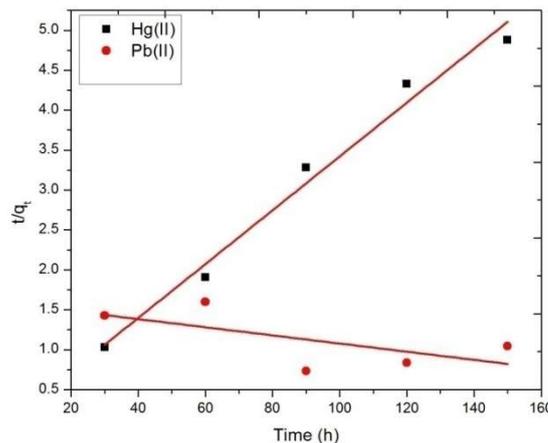

Fig.12. Pseudo-second order kinetic plots for adsorption of Pb (II) and Hg (II) onto PFCR

Pseudo-second order model

The pseudo-second order model is expressed as (Ho and Mckay, 1999):

$$\frac{t}{q_t} = \frac{1}{K_2 q_e^2} + \frac{t}{q_e} \qquad \text{………………..………. (12)}$$

Where, k_2 (g/mg/min) is the second order rate constant of adsorption. The plot of t/q_t versus t shows a linear relationship. Values of k_2 and equilibrium adsorption capacity q_e were calculated from the intercept and slope of the plot shown in Fig.12. The values of R^2 were greater than 0.983 for Hg (II) ion concentrations.

Intraparticle diffusion model

The intraparticle diffusion model (Mckay *et al.,* 1983) was used to identify the diffusion mechanism during adsorption process. It is described using the following equation

$$q_t = k_{id}t^{0.5} + C \qquad\qquad\qquad (13)$$

Where, k_{id} (mg g^{-1}min$^{-0.5}$) is the rate constant of the intraparticle diffusion model and C (mg/ g) reflects the boundary layer effect. The k_{id} and C can be determined from the slope and intercept of the linear plot of q_t against $t^{0.5}$. The pseudo-first order, pseudo-second order and intraparticle diffusion models were used to understand the kinetic nature of Pb(II) and Hg(II) onto PFCR adsorption system. All the values are presented in Table 5. All the experimental data showed better agreement with pseudo-second order model in terms of higher correlation coefficient value (R^2 >0.983), which suggested the adsorption rate of Hg(II) onto PFCR might be controlled by chemisorptions mechanism. The rate controlling step consisted valence forces through sharing or exchange of electrons between the adsorbent surface and adsorbate ions and no involvement of mass transfer in solution. The value of pseudo-second order rate constant, k_2, was 3.150 g/mg/min for Pb (II) was and 6.875 g/mg/min for Hg (II).

Table 5. Kinetic parameters for the adsorption of Pb(II) and Hg(II) on PFCR

Mathematical models	parameters	Pb(II)	Hg(II)
First order kinetics	R^2	0.019	0.392
	k_1 (min^{-1})	0.002	0.190
	q_e (mg/g)	889.2	2.238
Second order kinetics			
	R^2	0.416	0.983
	k_2 g/mg/min×10^{-3}	3.150	6.875
	q_e (mg/g)	200	30.30
Intra particle diffusion	R^2	0.887	0.903
	k_{id} g/mg/min$^{1/2}$	21.10	14.27
	C (mg/g)	100.1	56.34

Effect of temperature and thermodynamic data

The adsorption tests were performed by batch technique in single system at 308 K, 318 K, and 328 K, respectively. For kinetic studies, a series of 250 ml flasks were used and each flask was filled with PFCR at mass loadings 0.080 g for both Pb(II) and Hg(II) solution at 10 ppm metal solutions. The percentage removal of Pb(II) and Hg(II) are presented in Table 6 and Fig.13. The frequently used thermodynamic parameters assessed in this study are: change in Gibbs free energy (ΔG°), isosteric heat of adsorption (ΔH°) and the change in entropy (ΔS°) using VantHoff plot (Fig.14). The parameters are assessed using the equations (Biswas *et al.,* 2007).

$$K_L = \frac{q_e}{C_e} \qquad\qquad\qquad (14)$$

$$\Delta G° = -RT \ln K_L \qquad\qquad\qquad (15)$$

$$\ln K_L = \frac{\Delta S^0}{R} - \frac{\Delta H^0}{RT} \qquad\qquad\qquad (16)$$

Where, K_L is the Langmuir constants; C_e is the concentration of solute adsorbed on the resin at equilibrium, mg/ L. where R (8.314 J/mol K) is the gas constant, T (K) is the absolute temperature. The correlation coefficient for the linear plot for Pb (II) and Hg (II) was $R^2 = 0.962$ and $R^2 = 0.848$ respectively. Values of the standard Gibbs free energy change for the adsorption process obtained from Eq. (15) were listed in Table 7.

Table 6. Effect of temperature

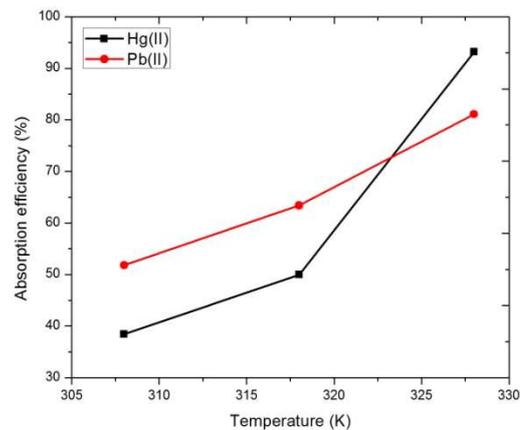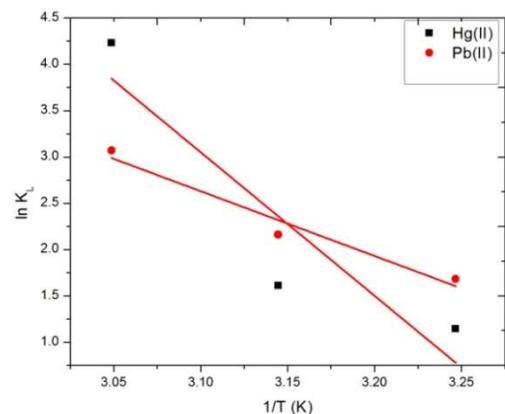| Metal ions	Adsorption Efficiency (%)			Amount of adsorbed (q) (mg/g)		
	308 K	318 K	328 K	308 K	318 K	328 K
Hg (II)	38.4	50.0	93.2	48.5 ×10^2	63.0 ×10^2	117.0 ×10^2
Pb (II)	51.8	63.4	81.1	93.5 ×10^2	114.5 ×10^2	146.5 ×10^2

Fig.13. Effect of temperature

Fig.14. Van't Hoff plots of ln K_L versus 1/T for the adsorption of Hg(II) and Pb(II) onto PFCR

Table 7. Thermodynamic parameters for the adsorption of Pb(II) and Hg(II) on PFCR

Dyes	Thermodynamics parameters					
	R^2	ΔH° J/mol	ΔS° J/mol K	-ΔG°(kJ/mol)		
				308K	318K	328K
Hg(II)	0.848	128.7	424.5	2920.9	4254.9	11538.8
Pb(II)	0.962	58.09	201.9	4305.5	5711.4	8371.8

It is well known that these parameters can evaluate the orientation and feasibility of the physicochemical adsorptive reaction. The negative adsorption standard free energy changes

(ΔG°) at all temperatures indicated that the adsorption of Pb(II) and Hg(II) on PFCR was a general spontaneous process. In addition, the positive enthalpy change (ΔH°) values indicated that the Pb(II) and Hg(II) adsorption on PFCR was an endothermic process. The positive value of the (ΔS°) implies the increment of an orderliness between the adsorbate and the adsorbent molecules.

Conclusion

In this study, PFCR composite was prepared, characterized and used as a bioadsorbent. PFCR has higher adsorption capacity for Hg(II) and Pb(II) due to the introduction of β-cyclodextrin. The adsorption of Hg(II) and Pb(II) onto PFCR followed Jovanoic isotherm and was spontaneous and endothermic in nature. Batch adsorption experiments showed that the adsorption process followed the pseudo-second-order kinetic model. The novel PFCR can be utilized as an environment-friendly bioadsorbent for the removal of metals from aqueous solution due to the efficient and fast adsorption process, as well as simple and convenient separation.

REFERENCES

Albert, M., Demesmay, C., and Rocca, J.L., 1995. Analysis of organic and nonorganic arsenious or selenious compound by capillary electrophoresis, *Fresenius. J. Anal. Chem.*, 351: 126-432

Aroua, M.K., Leong, S.P.P., Teo, L.Y., Yin, C.Y., and Daud, W.M.A.W., 2008. Real-time determination of kinetics of adsorption of lead(II) onto palm shell-based activated carbon using ion selective electrode, *Bioresour. Technol.,* 99(13): 5786-5792

Badruddoza, A. Z. M., Tay, A. S. H., Tan, P. Y., Hidajat, K., and Uddin, M. S., 2011.Carboxymethyl-β-cyclodextrin conjugated magnetic nanoparticles as nano-adsorbents for removal of copper ions: synthesis and adsorption studies. *J.Hazard.Mater.,*185(2- 3): 1177-1186.

Balaria, A., Schiewer, S., and Schiewer, S. 2008. Assessment of biosorption mechanisms for Pb binding by citrus pectin, *Sep. Purif. Technol.,* 63: 577-581

Biswas, K., Saha, S.K., and Ghosh, V.C., 2007. Adsorption of Fluoride from Aqueous Solution by a Synthetic Iron(III)−Aluminum(III) Mixed Oxide, *Ind. Eng. Chem. Res.,* 46(16): 5346- 5356

Crini, G., 2005. Recent developments in polysaccharide-based materials used as adsorbents in wastewater treatment, *Progress in Polymer Science.* 30(1): 38-70

Crini, G., and Peindy, H. N. 2006. Adsorption of C.I. Basic Blue 9 on cyclodextrin-based material containing carboxylic groups, *Dyes and Pigments.,* 70(3): 204-211

Denizli, A., Senal, S., Alsancak, G., Tuzmen, N.,and Say, R. 2003. Mercury removal from synthetic solutions using poly(2-hydroxyethylmethacrylate) gel beads modified with poly(ethyleneimine)*, React. Funct. Polym.,* 55(2): 121-130.

Dubinin, M.M., and Radushkevich, L.V. 1947.Equation of the Characteristic Curve of Activated Charcoal, *Proc. Acad. Sci, USSR.,* 55: 331-333

Feng, Y., Gong, J. L., Zeng, G. M., Niu, Q. Y., Zhang, H. Y., and Niu, C. G., 2010. Adsorption of Cd (II) and Zn (II) from aqueous solutions using magnetic hydroxyapatite nanoparticles as adsorbents, *Chem. Eng. J.,*162: 487-494

Foo, K.Y., and Hameed, B.H., 2010.Insights into the modeling of adsorption isotherm systems, *Chem. Eng. J.,* 156(1): 2-10

Guo, Y., Qi, J., Yang, S., Yu, K., Wang, Z., and Xu, H. 2002. Adsorption of Cr (VI) on micro-and mesoporous rice husk-based activated carbon, *Mat. Chem. Phys.*, 78: 132-137

Gupta, N ., Kushwaha, A.K.,and Chattopadhyaya, M.C. 2012. Adsorptive removal of Pb^{2+}, Co^{2+} and Ni^{2+} by hydroxyapatite/chitosan composite fro m aqueous solution, *J.Taiwan. Instit. Chem.Eng.,* 43(1): 125-131

Gupta, V.K., Jain, R., Mittal, A., Mathur, M., and Sikarwar, S., 2007. Photochemical degradation of the hazardous dye Safranin-T using TiO_2 catalyst, *J.Colloid and Interface Sci,.* 309(2): 464-469.

Hall, K.R., Eagleton, L.C., Acrivos, A., and Vermilion, T., 1966. Pore- and Solid-Diffusion Kinetics in Fixed-Bed Adsorption under Constant-Pattern Conditions, *Ind.Eng.Chem.Fund.,* 5(2): 212-223.

Ho, Y.S., and Mckay, G., 1999. Pseudo-second order model for sorption processes, *Process Biochem.,* 34: 451-465

Ireland, M.P., 1991. *Biological Monitoring of Heavy Metals*, Wiley, New York.

Jovanoic, D.S., 1969. Physical adsorption of gases, *Colloid. Polym. Sci.,* 235(1): 1203-1213.

Lagergren, S., 1898. Zur theorie der sogenannten adsorption gelöster stoffe, *Kungliga Svenska Vetenskaps-Akademiens Handlingar,* 24 (4):1-39

Mahlambi, M. M., Malefetse, T. J, Mamba, B. B., and Krause, R.W., 2010. β-Cyclodextrin-ionic liquid polyurethanes for the removal of organic pollutants and heavy metals from water: synthesis and characterization, *J.Poly.Resear.,* 17: 589-600.

Martins, B.L., Cruz, C.C.V., Luna, A.S., and Henriques C.A. 2006. Sorption and desorption of Pb^{2+} ions by dead Sargassum sp. Biomass, *Biomass.Biochem. Eng.J.*, 27(3): 310-314

Mckay, G., Blair, H.S., and Gardner, J. 1983. The adsorption of dyes in chitin. III. Intraparticle diffusion processes, *J. Appl. Polym. Sci.,* 28(5): 1767-1778

Merzouka, B., Gourich, B., Sekki, A., Madani, K., and Chibane, M. 2008. Removal turbidity and separation of heavy metals using electrocoagulation-electroflotation technique A case study, *J. Hazard. Mater.* 164(1):215-220.

Meunier, N., Drogui, P., Montan´e, C., Hausler, R., Mercier, G.,and Blais J.F., 2006.Comparison between electrocoagulation and chemical precipitation for metals removalfrom acidic soil leachate. *J.Hazard. Mater.B* 137: 581-590

Mittal, A, Gupta, V, Malviya, A., and Mittal, J. 2008. Process development for the batch and bulk removal and recovery of a hazardous, water-soluble azo dye (Metanil Yellow) by adsorption over waste materials (Bottom Ash and De-Oiled Soya). *J. Hazard. Mater.*151 (2–3): 821-832.

Mohamed, M., Mohand, S.O., Marc, L., and Louis, C.M. 2008. Removal of lead from aqueous solutions with a treated spent bleaching earth, *Hazard. Mater.* 159(2-3): 358-364

Ngah, W.S. W., Endud, C.S. and Mayanar, R. 2002. Removal of copper(II) ions from aqueous solution onto chitosan and cross-linked chitosan beads, *React. Funct. Polymer.* 50: 181-190

Norkus, E., 2009. Metal ion complexes with native cyclodextrins. An overview, *J. Inclu. Phenomena and Macro. Chem.,* 65(3-4): 237-248.

Nuhoglu, Y., Malkoc, E., Guurses, A., and Canpolat, N. 2002. The removal of Cu(II) from aqueous solutions by *Ulothrix zonata, Bioresour. Technol.,* 85(3): 331-333

Szejtli, J. 1998. Introduction and General Overview of Cyclodextrin Chemistry. *Chemical Reviews.,* 98(5): 1743-1754

Temkin, M.J., and Pyzhev, V. 1940. Kinetics of Ammonia Synthesis on Promoted Iron Catalysts. Acta Physicochim Acta. *Physiochim URSS.,* 12: 217-222

****